**SpringerPlus manuscript No.**
(will be inserted by the editor)

# Power Flow Analysis and Optimal Locations of Resistive Type Superconducting Fault Current Limiters

**X. Zhang · H. S. Ruiz · J. Geng · B. Shen · F. Lin · H. Zhang · T. A. Coombs**

Received: 31 March 2016 / Accepted:

**Abstract** Based on the conventional approaches for the integration of resistive-type superconducting fault current limiters (SFCLs) on the electric distribution networks, SFCL models largely rely on the insertion of a step or exponential resistance that is determined by a predefined quenching time. In this paper, we expand the scope of the aforementioned models by considering the actual behaviour of a SFCL in terms of the temperature dynamic power-law dependence between the electrical field and the current density, characteristic of high temperature superconductors. Our results are compared with the step-resistance models for the sake of discussion and clarity of the conclusions. Both SFCL models were integrated into a power system model built based on the UK power standard, and the impact of these protection strategies on the performance of the overall electricity network was studied. As a representative renewable energy source, a 90 MVA wind farm was considered for the simulations. Three fault conditions have been simulated, and the figures for the fault current reduction predicted by both fault current limiting models have been compared in terms of multiple current measuring points and allocation strategies. Consequently, we have shown that the incorporation of the $E - J$ characteristics and thermal properties of the superconductor at the simulation level of electric power systems, is crucial for reliability estimations and optimal location of resistive type SFCLs in distributed power networks. Our results may help to the decision making by the distribution network operators about investment and promotion of the SFCL technologies, as a maximum number of SFCLs for different fault conditions and multiple locations has been determined.

**Keywords** Superconducting fault current limiter · distributed power system · short-circuit current · optimal location

X. Zhang, J. Geng, B. Shen, F. Lin, H. Zhang, and T. A. Coombs
Department of Engineering, University of Cambridge, 9 JJ Thomson Avenue, Cambridge, CB3 0FA, United Kingdom
E-mail: xz326@cam.ac.uk

H. S. Ruiz
Department of Engineering, University of Leicester, University Road, Leicester, LE1 7RH, United Kingdom
E-mail: dr.harold.ruiz@leicester.ac.uk

## 1 Introduction

With the persistent increase of conventional system generation and distributed generations (DGs), such as, photovoltaic plants, concentrating solar power plants, and wind farms, the likelihood of fault events capable to cause great and irreparable damage to a large set of electrical devices, or even system blackout, has been rapidly rising [1,2]. Various strategies for mitigating the fault current levels have been implemented in the power industry, such as, construction of new substations, split of existing substation busses, upgrade of multiple circuit breakers, and installation of high impedance transformers. Nevertheless, all these operational practices involve a not negligible degradation of the systems stability and their performance, what ultimately means the occurrence of significant economic losses and further investment [3]. Series reactors and solid state fault current limiters are also widely used although these insert a high impedance causing a continuous voltage drop and power losses during normal operation [4]. However, the superconducting fault current limiting technology can stand up for all these difficulties preserving the stability and reliance of the power system with minimum losses

at normal conditions. An exhaustive review on the successful field test and different existing numerical models of SFCLs can be found in Ref. [5].

For performance simulation of SFCLs installed in real power grids, two simplified SFCL models have been identified as of common use. The first approach was to model the SFCL as a step-resistance with pre-defined triggering current, quench time, and recovery time as in Ref. [6] and Ref. [7]. This approach allows to consider a simplified scenario where no energy loss occurs during the superconducting state, and a high impedance is considered for modelling its normal state, by ensuring that the SFCL responds to faults in an instantaneous fashion. However, it may lead to significant inaccuracies since the quenching and recovery characteristics depend on the thermal and electrical properties of the superconductors, which are both neglected in this case. On the other hand, the modelling of a SFCL into a power grid can also be simplified by using an exponential function for the dynamic resistance of the SFCL device, in which the quenching action of the superconducting material is solely determined by time. This method has been previously implemented in Refs. [8] and [9] in order to study the optimal location and associated resistive value of SFCLs for a schematic power grid with an interconnected wind-turbine generation system, finding that the installation of SFCLs cannot only reduce the short-circuit current level but also, it can dramatically enhance the reliability of the wind farm. Compared with the Heaviside step function derived from the previous approach, this exponential resistance curve fits better with the real performance of the SFCL and furthermore provides aggregated computational benefits in terms of numerical convergence. Nevertheless, the SFCL characteristics including triggering current, quenching, and recovery time also have to be set before initialising the simulation, i.e., under this scenario also the physical properties of the superconductors are ignored. On the other hand, a more advanced model for resistive-type SFCL was presented in Ref. [10] where both the physical properties and the real dimensions of superconductors were considered. A similar model was then built by D. Colangelo et al.,[11] in order to simulate the behaviour of the SFCL designed in the ECCOFLOW project. Using this model the quenching action of the SFCL is no longer pre-defined. However, within these models the computational complexity is significantly increased, especially during large scale power network simulation. Hence, during performance simulation of SFCLs installed in power systems, it is rather important to study the necessity of considering thermal and electrical properties of superconducting materials, in order to be able to choose a better side between the tradeoff of computational complexity and model accuracy. Furthermore, it is worth noticing that for any of the adopted strategies, the research must ultimately addresses the finding of the optimal location of multiple SFCLs inside the power network, which as far of our knowledge it has been done by considering a maximum of just two SFCLs, which means that the cooperation and prospective need of more SFCLs remains as an open issue.

In this paper we present a comprehensive study about the performance and optimal location analysis of resistive type SFCLs in realistic power systems, starting from the simplest consideration of a single step-resistance for the activation of the SFCL, up to considering the actual electro-thermal behaviour of the superconducting component. We have simulated the performance of the SFCL under the scheme provided by two different models: (i) as a nonlinear resistance depending on time and, (ii) as a dynamic temperature-dependent model with the actual $E - J$ characteristics of the superconducting material. The applied power grid model which has interconnected dispersed energy resource was built based on the UK network standard. Through the simulations of the system behaviours under three fault conditions (two distribution network faults in different branches, and one transmission system fault), the optimum SFCL installation schemes were found from all the feasible combinations of SFCLs. In addition, a detailed comparison between the figures obtained for each one of the above mentioned cases has been performed, proving that the nonlinear resistor model is insufficient for an accurate estimation of the reliability figures and optimal location of the SFCL, as the complex thermal and electrical behaviours of the superconducting material during its transition to the normal state cannot be simplified to a single step-resistance.

This paper is organised as follows. Section 2 introduces the topology of the power system and proposed SFCL models. In Section 3 a comprehensive reliability study on the SFCL scheme, including the analysis of the network stability, current limiting performance, and recovery characteristics of the SFCL with and without the inclusion of a bypass switch is presented. Then, a novel method about how to determine the optimal location of multiple SFCLs in a large scale electrical grid is the described in Section 4. Finally, the main conclusions of this paper can be found in Section 5.

## 2 SFCLs and topology of the power system

The upfront topology of the modelled power system depicted in Fig. 1 has been built based on the UK

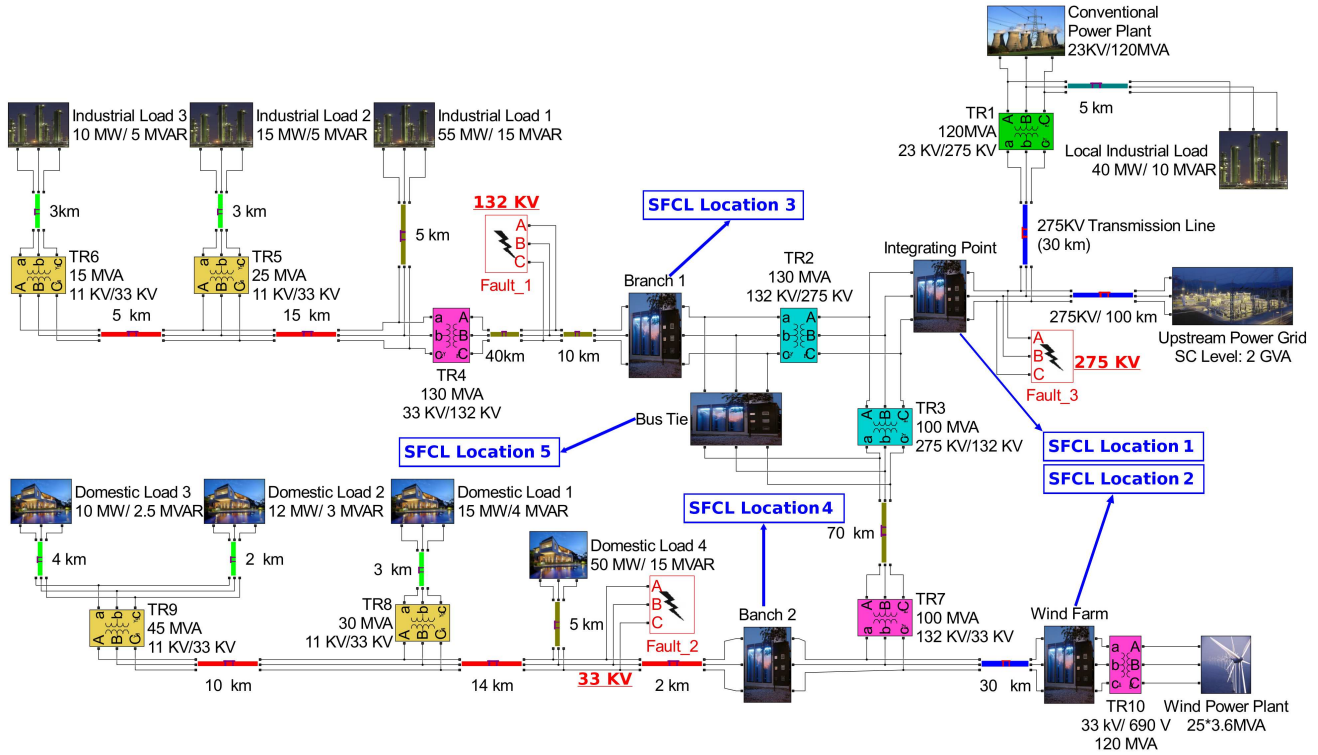


**Fig. 1** Power system model based on the UK grid standard as described in Section 2. Three prospective fault positions and five prospective SFCL locations are illustrated.

network standards [12]. The power system has a 120 MVA conventional power plant emulated by a three-phase synchronous machine, which is additionally connected to a local industrial load of 40 MW located 5 km away from the main power plant. Afterwards, the voltage level is boosted from 23 KV to 275 KV by a step-up transformer (TR1), from where the conventional power plant is connected to an upstream power grid rated with a short circuit level of 2GW through 130 km long distributed-parameters transmission line. Then, the 275 KV high-voltage transmission system is split into two distribution networks. First, after voltage level stepped down to 33 KV by substations TR2 and TR4, the upper branch (industrial branch) supplies power to three industrial loads which rated power are 55 MW, 15 MW, and 10 MW, separately. Likewise, the lower branch (domestic branch) is also connected to two step-down substations TR3 and TR7, with 70 km distance between them. The role of these two substations is reduce the voltage of the lower sub-grid to 33 KV, as it is the same voltage level rated by the interconnected 90 MVA wind power plant, which emulates the Rhyl Flats offshore wind farm located in North Wales, after being boosted by TR10. This offshore wind power plant is composed of twenty-five fixed-speed induction-type wind turbines each having a rating of 3.6 MVA, and it is located 30 km away from its connecting point with the lower distribution network [13]. After integration, the lower branch and the wind farm together provide electric energy to four domestic loads with rated power of 50 MW, 15 MW, 12 MW and 10 MW, separately. Finally, the industrial branch and the domestic branch are connected through a bus-bar coupler, and the power system is balanced in a way that the current flowing through the bus-tie is only of a few amperes during normal operation.

It is generally accepted that the three-phase (symmetric) short-circuit fault provokes the highest fault current among all possible faults, since it will cause the most drastic decrease of the system impedance. In order to ensure safe operation, the maximum current and electrodynamic withstand capabilities of electrical equipment are primarily designed according to this situation. Therefore, it is essential to simulate the behaviour of the power system under three-phase short-circuit fault. The symmetric faults were initialised at three potential locations marked as Fault 1 (132 KV), Fault 2 (33 KV) and Fault 3 (275 KV), which represent prospective faults occurring at the industrial branch, the domestic branch, and the transmission system, respectively (see Fig. 1). Five positions for the installation of SFCLs are proposed as shown in Fig. 1, namely

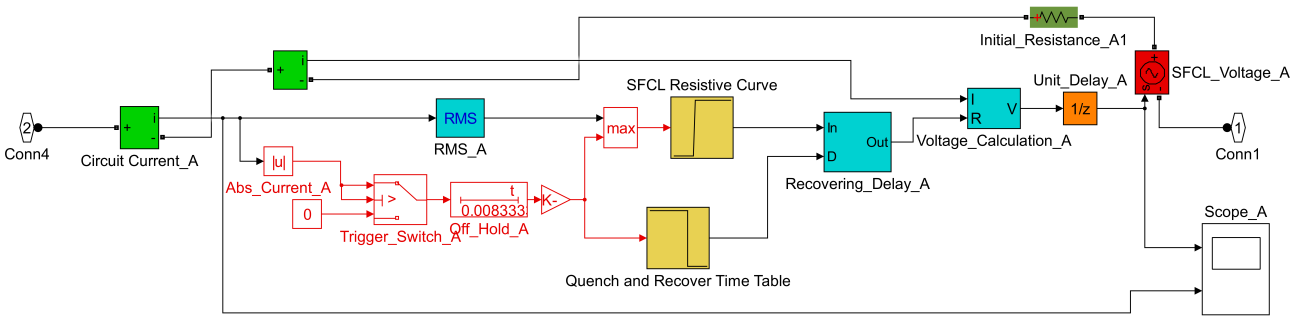


**Fig. 2** One Phase of the step resistance SFCL model.

at: (i) the integrating point between the conventional power plant and the upstream power grid (Location 1), (ii) the interconnection between the wind farm and the port of domestic branch (Location 2), (iii) the industrial loads branch (Location 3), (iv) the domestic loads branch (Location 4), and (v) the bus-tie coupling the two distribution networks (Location 5).

On the other hand, identical single phase SFCLs are implemented for each one of the three phases of the system, as each phase of the SFCL would only be triggered by the current flowing through its own phase. However, under symmetric faults, each phase of the SFCL will quench slightly asynchronously within the first cycle of the fault current, leading to an instantaneous unbalance between the phases [14]. Hence, for all types of faults and at diverse locations, independent modules for each one of the three phases have been considered, it in order to allow an accurate simulation of the SFCL's effects on the overall power grid. Two different models have been considered in order to emulate the SFCL performance, as described below.

### 2.1 Step Resistance SFCL

Current limiting performance of the developed step resistance SFCL model is dominated by five predefined parameters: (i) triggering current, (ii) quenching resistance, (iii) quenching time, which has been assumed equals to 1 ms accordingly with Refs. [15] and [16], (iv) a normal operating resistance of 0.01 $\Omega$ and, (v) a recovery time of 1 s. The values of triggering current and quenching resistance are not provided in this section since they vary with the location of the SFCL. The structure of the step resistance model is illustrated in Fig. 2.

The operating principle of this model can be summarised as follows: first, the SFCL model calculates both the absolute and RMS values of flowing current. If both values are lower than the triggering current, the model will consider the SFCL in superconducting state and insert normal operating resistance (0.01 $\Omega$) into the grid. On the contrary, if either the absolute value or the RMS value of a passing current exceeds the triggering current level, the output resistance will be increased to the quenching resistance after the predefined quenching time. Lastly, if current flowing through the SFCL model falls below the triggering current due to the clearance of the fault, the SFCL will restore its superconducting state after the recovery time.

### 2.2 SFCL with E-J-T power law

The sudden change in the SFCL resistance can be macroscopically simplified into the so-called $E-J$ power law [25], which can be divided into three sub-regions: superconducting state, flux flow state, and normal conducting state [10,14,26]. All three sub-regions follow different power laws, combination of which forms the entire $E-J$ characteristics of the SFCL as follows:

$$E(T,t)=\begin{cases} E_c\left(\dfrac{J(t)}{J_c(T(t))}\right)^n, & \text{for } E(T,t)<E_0 \text{ and } T(t)<T_c,\\ E_0\left(\dfrac{E_c}{E_0}\right)^{m/n}\left(\dfrac{J_c(77K)}{J_c(T(t))}\right)\left(\dfrac{J(t)}{J_c(77K)}\right)^m, & \text{for } E(T,t)>E_0 \text{ and } T(t)<T_c,\\ \rho(T_c)\dfrac{T(t)}{T_c}J(t), & \text{for } T(t)>T_c, \end{cases} \tag{1}$$

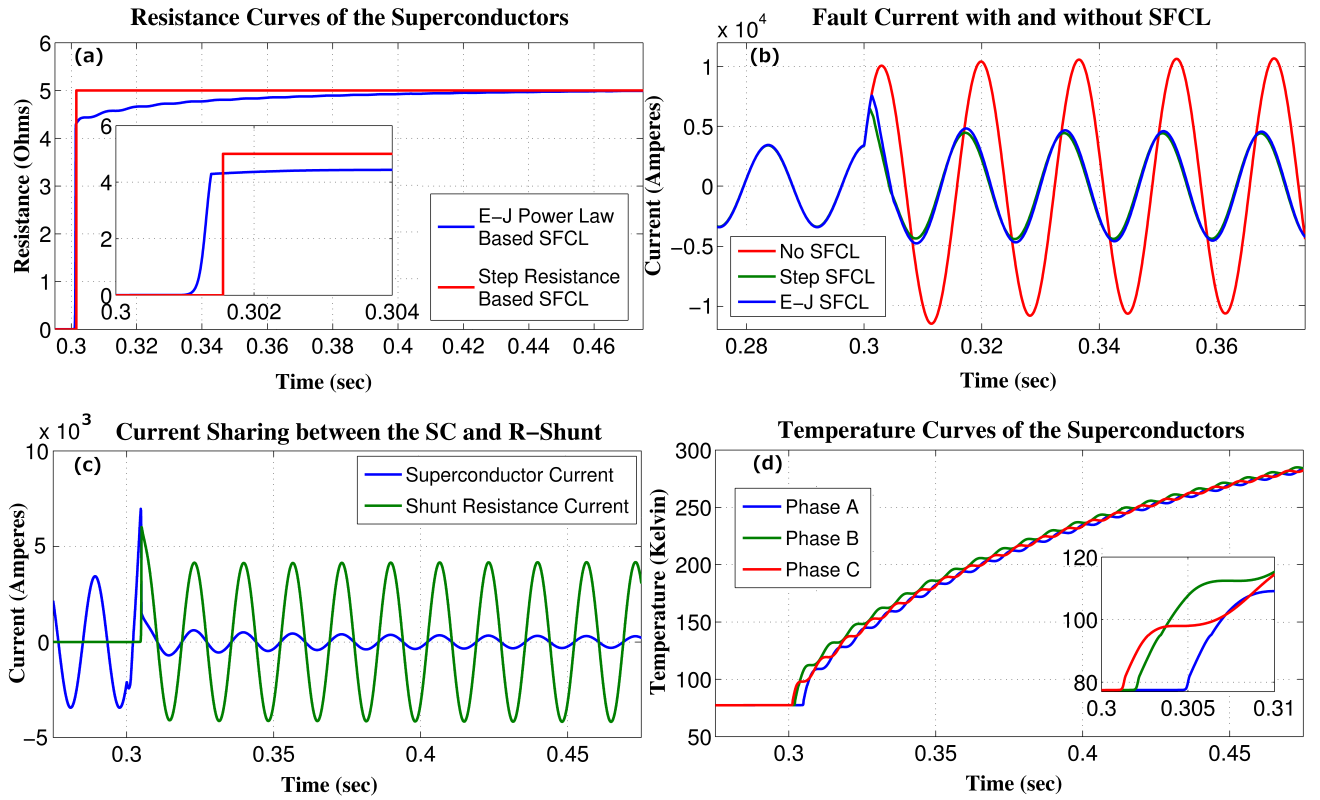


**Fig. 3** (Color Online) Performance comparison between the step SFCL model and the $E-J$ power law based SFCL model. The displayed insets in subplots (a) and (d) are measured in the corresponding units of the main plot.

where,

$$J_c(T(t)) = J_c(77K)\frac{T_c - T(t)}{T_c - 77}, \quad for \quad J > J_c. \tag{2}$$

On the one hand, for the modelling of the SC state we have used $n = 9$ in accordance with Refs. [17–21], and $m = 3$ for the flux flow state in good agreement with the experimental data reported in Refs. [22] and [23]. On the other hand, we have assumed the normal conducting state resistivity as a linear function of temperature when $T(t) > T_c$, with $\rho(T_c) = 7 \times 10^{-6}\Omega$ for Bi2212 [24]. Furthermore, the relationship between the critical current density and the temperature is also set to be linear as in Eq.(2), as it has been proved by S. Kozak et al. for the specific case of Bi2212 compounds [27]. In addition, for completing the SFCL model, a CuNi alloy ($\rho = 40\mu\Omega \cdot m$) resistor is connected in parallel with the superconductor on the basis of the project disclosed in Ref. [28]. This shunt resistance can protect the superconducting material from being damaged by hot spots that are developed under limiting conditions, and furthermore prevents over-voltages that possibly appear if the quench occurs too rapidly [29,30]. Finally, by assuming that the SC composite is homogeneous, the thermal modelling of the SFCL considers the first order approximation of the heat transfer between the superconductor and the liquid nitrogen bath as follows:

$$R_{SC} = \frac{1}{2\kappa\pi d_{SC} l_{SC}}\ , \tag{3}$$

$$C_{SC} = \frac{\pi d_{SC}^2}{4} l_{SC} c_v\ , \tag{4}$$

$$Q_{generation}(t) = I(t)^2 \times R_{SFCL}(t)\ , \tag{5}$$

$$Q_{cooling}(t) = \frac{T(t) - 77}{R_{SC}}\ , \tag{6}$$

where $R_{SC}$ stands for the thermal resistance from the SC material to its surrounding coolant, $C_{SC}$ is the specific heat of Bi2212 [31], $c_v = 0.7 \times 10^{-6} J/(m^3 \cdot K)$, and

$$T(t) = 77 + \frac{1}{C_{SC}} \int_0^t [Q_{generated}(t) - Q_{cooling}(t)]dt\ . \tag{7}$$

The SC is modelled as a cylindrical wire of length $l_{SC}$, which is adjusted at each installing location in order to limit the prospective fault current to the desired level. Likewise, the diameter $d_{SC}$ is regulated to ensure that the SFCL not only remains into the superconducting state during normal operation, but also quenches

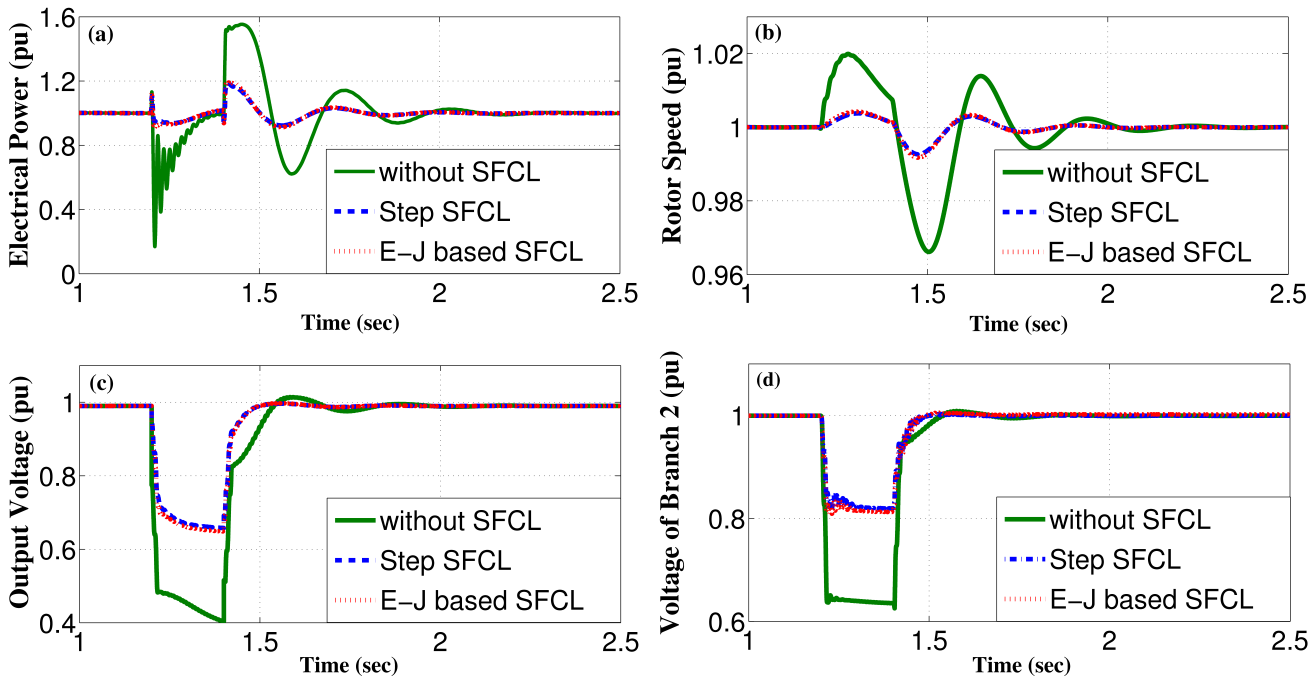


**Fig. 4** (Color Online) Generator parameters and voltage of branch 2 in response to a 200 ms three-phase to ground fault at branch 1.

within a few milliseconds once a short-circuit fault occurs at some location into the grid. In practice, despite the wire diameter cannot be modified after fabrication, one can connect several wires in parallel to achieve the expected current limiting performance [32], which allow us to use the previous approaches.

## 3 Network stability, current limiting performance, and recovery characteristics

In order to compare the fault current limitation properties of the two SFCL models, in Fig. 3 we present the results for a three-phase to ground fault with negligible fault resistance when it is initialised at the domestic network (Fault 2), and a single SFCL is installed next to the fault position (Location 4). Fig. 3(a) illustrates that the step resistance model and the $E-J$ power law based model both respond almost simultaneously to the occurrence of a short-circuit fault. However, as the SFCL needs $\sim 2$ ms to fully quench due to its $E-J$ characteristic and dynamic temperature (Fig. 3(d)), the first peak reduction gained onto the step resistance model is overestimated by 11% (7.6 kA and 6.5 kA for the two SFCL models, respectively. 10 kA without SFCL), as shown in Fig. 3(b). In addition, the shunt resistor diverts the major portion of the fault current after the superconductor develops its normal state (Fig. 3(c)). Therefore, the shunt resistance effectively lowers the thermal stress on the HTS wire, simultaneously preventing damages by overheating, whilst the recovery time is reduced [33].

Initial tests without integration of the SFCL model have confirmed that the power system operates at rated state during normal operation. Then, under occurrence of three-phase to ground faults at Fault-1, Fault-2 and Fault-3 (see Fig. 1), the short-circuit currents were measured at the integrating point (Location 1), wind farm (Location 2), branch 1 (Location 3) and branch 2 (Location 4), such that the instantaneous fault current can be described by:

$$i_k = \underbrace{I_{pm} sin(\omega t + \alpha - \beta_{kl})}_{\text{periodic component}} + \underbrace{[I_m sin(\alpha - \beta)] - I_{pm} sin(\alpha - \beta_{kl})]e^{-\frac{t}{\tau_k}}}_{\text{aperiodic component}} , \quad (8)$$

where $I_m$ is the amplitude of the rated current of the power grid, $\phi$ and $\phi_{kl}$ represent the impedance angles before and after the fault, respectively; $\alpha$ defines the fault inception angle, $I_{pm}$ states the magnitude of periodic component of the short-circuit current, and $\tau_k$ stands for the time constant of the circuit. Hence, the fault currents achieve their maximum values when $\alpha - \beta_{kl} = \pi(n+1)/2$ with $n \in \mathbb{Z}$, and this condition is implemented all through our study in order to consider

the most hazardous fault scenarios, and the impact of the SFCLs on the generation side and voltage stability of the grid. For instance, when a 200 ms three-phase to ground fault is applied at the industrial branch (Fault-1), after 1.2 s within normal operating conditions, the response of the output electrical power, rotor speed, and terminal voltage for the conventional power plant (23 KV / 120MVA), and the voltage output at the domestic branch (Branch 2) are shown in Fig. 4.

Initially we have to consider the power system operation without the insertion of SFCLs. Under this scenario, the output electrical power drops sharply to 0.15 *pu* just after the fault incident (Fig. 4(a)), whilst the governors of the power plant such as steam and hydro still contribute with the same mechanical power to the rotors. Thus, a rapid acceleration of the rotors occurs due to this power imbalance, as it is shown in Fig. 4(b). However, when a SFCL is installed at Branch 1 (Location 1), its high resistance state facilitates the SFCL to dissipate the excess generator power during the fault condition, hence improving the energy balance of the system and reducing the variation of the rotor speed effectively. Furthermore, with consideration of the conventional equal-area criterion for stability issues [15] [34], the SFCL could improve the damping characteristics of generator speed, system frequency, as well as the system current, as the insertion of the high resistance into the grid would significantly increase the damping ratio. Moreover, due to the short-circuit fault of Branch 1, a sharp voltage drop (Figs. 4 (c) - (d)) can be seen at both the power plant terminal (0.5 *pu*) and the non-faulted Branch 2 (0.35 *pu*). Then, by introducing the SFCL which acts as a voltage booster, the observed voltage dips are mitigated by 40% and 50%, respectively. This improvement allows the healthy parts of the system (without the fault inception) to be less affected and, makes the use of a SFCL a reliable fault ride-through scheme.

Moreover, it is worth noting that without the protection of the SFCL a 200 ms short-circuit fault was initiated in Branch 1 (Fault 1) in order to study the relationship between the current limiting performance of SFCL and the maximum normal resistance. Firstly, without the protection of the SFCL, simulation results have shown that the first peak of current flowing into Branch 1 reaches $\sim$ 3.8 kA, which means $\sim$ 6.8 times higher than the rated value (560 A). Then, after installation of the SFCL a considerable reduction of the fault current is observed as shown in Fig. 5. The insets (a) and (b) on this figure illustrate the variation of the limited current when the two SFCL models (step resistance, and $E-J-T$ power law) are integrated at Branch 1 (Location 3).

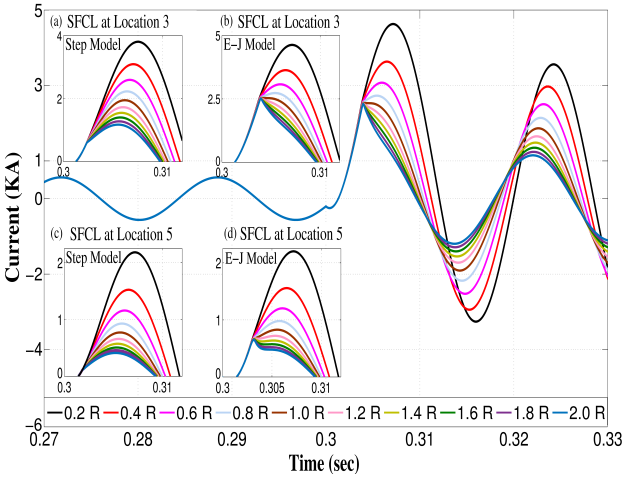


**Fig. 5** (Color Online) Current curves of phase A under branch 1 faulted (Fault 1) when the SFCL resistance increases from 0.2 R to 2.0 R.

Within the step-resistance model, with the SFCL resistance increasing from 0.2 R to 2 R ($R = 30\Omega$) during the quenched state, the peak value of the fault current gradually decreases from $\sim$ 3.8 kA to $\sim$ 1.2 kA, showing a small displacement of the peak values. However, in the case of the $E-J-T$ power law model, a noticeable *kink* appears at 2.5 kA, when the maximum resistance of the SFCL is greater than 1 $R$. Remarkably, this distinctive *kink* can be interpreted as the threshold value for the maximum reduction of the fault current for a SFCL which cannot be determined with any other model as far of the knowledge of the authors. To illustrate the difference, the readers can notice that the step-model resistance predicts a continuous decrease on the first peak of the fault current as $R$ increases (Fig. 5 (a) & (c)), contrary to what is observed with the more realistic $E-J-T$ model (Fig. 5 (b) & (d)), which predicts that no matters the increment of the SFCL resistance, after certain value it can only limit the first peak of the fault current to a well defined threshold. For instance, for the case illustrated in Fig. 5, we have determined that on the instant that the *kink* appears, the current curves overlap at about 2.5 kA, defining hence, the maximum peak reduction of the fault current at this location (Location 3), and therefore an optimal SFCL resistance. It is worth mentioning that the characteristic kink is also observed when the SFCL is located at any other position, e.g., at the bus-tie (Fig. 5 (c) & (d)), which validate the generality of our statement. Thus, in terms of economic figures, it represents a very valuable result for the distribution operators as it allows to state a maximum threshold on the required size for the SFCL's capacity, minimising material investments for the specific locations as beyond this threshold no further

reduction of the first peak of the fault currents can be achieved.

On the other hand, although the passive transition of the SC material and the high normal resistance enables the SFCL to limit the fault current before attaining its first peak, in some cases the recovery characteristics of the SFCL need to be improved because the SC may need several minutes to restore its superconducting state under load conditions. For instance, if a fault event quenches a single SFCL located at the domestic branch, it will then may take more than 300 seconds to recover once the fault current has been cleared. Therefore, in order to decrease the recovery time of the SFCL we have connected a bypass switch parallel to both the SC and the shunt resistance [35]. Thus, when the SFCL can fastly recover the superconducting state under load conditions, the switch $S1$ remains closed after the fault is cleared. However, if the SFCL cannot be automatically recovered within a few seconds then, the switch $S2$ can be closed and the switch $S1$ is instantaneously opened to quickly disconnect the SC from the system. Thereby, it allows the SC to start its recovery process without further accumulation of heat, as it is shown in Fig. 6 for a SFCL installed at location 2 after encountering a 0.2 s three-phase to ground fault at the domestic branch (Fault 2). It is worth mentioning that for this case, and without applying the bypass switch strategy, certain amount of current continue passing through the SFCL after the clearance of the fault. This flow of current keeps generating heat inside of the superconductor, what significantly slows down the decrease of temperature, and hence delay the recovery of the SFCL by more than five minutes. However, with a properly designed control scheme, the $E-J-T$ model can open the switch $S1$ and close the switch $S2$ at the moment that the fault ends, thus transferring the current to the $S2$ branch. In fact, by using this method we have determined that the recovery time can be reduced to less than 1.6 s without affecting the normal operation of the power grid. Then, after the SC is restored to its superconducting state, the switches $S1$ and $S2$ act again preparing the SFCL for the next fault. However, as it is no possible to foresee the location of a fault event, the optimal location for the installation of one or multiple SFCLs has to be assessed, being this the purpose of the following section.

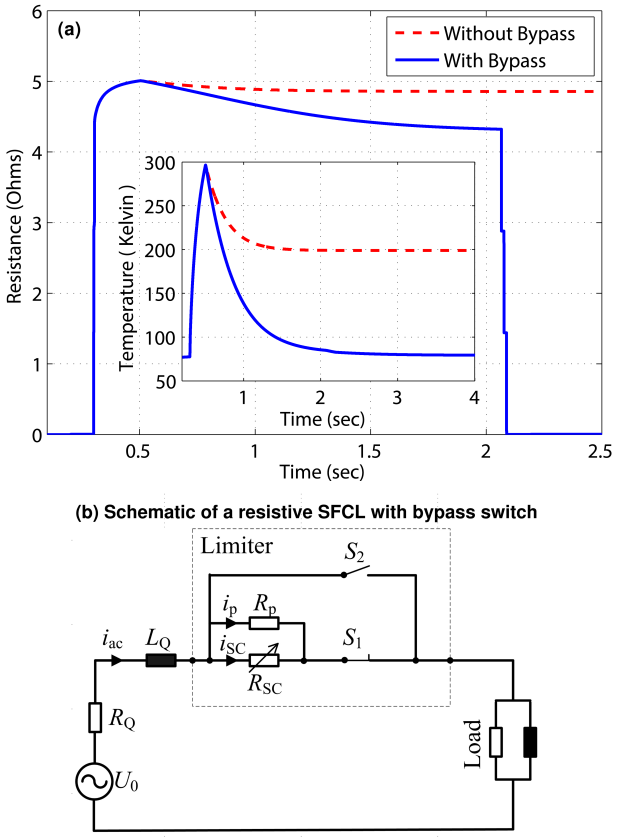


**Fig. 6** (Color Online) SFCL resistance and temperature dynamics with and without the assistance of the Bypass switch strategy shown in the bottom of the figure.

## 4 Identification of the Optimal Location

In order to attain an accurate estimation of the optimal location for the installation of one or multiple SFCLs, all possible SFCL combinations according to the five proposed locations depicted in Fig. 1, have been analysed for three different fault points. It results in a total of 31 allocation strategies, including five different schemes for the integration of a single SFCL (Locations 1 to 5), 10 dual combinations of SFCLs, 10 further combinations of three SFCLs, five scenarios where four SFCLs are working together, and finally the cooperation between all five SFCLs.

The current signals at both wind farm terminal (Location 2) and the integrating point of conventional power plant and upstream power grid (Location 1) were measured for all three fault conditions (Fig. 1). Moreover, we have analysed the current injection of industrial branch (Location 3) and domestic branch (Location 4) when faults happen at the two networks, Fault 1 and Fault 2, respectively. For the sake of brevity, we do not present the results for the measured current at the industrial branch when the Fault 2 or Fault 3 occurs, because based on the analysis of the system impedance change, the magnitude of the current flowing into the industrial branch is actually reduced by the two faults to levels lower than the normal current, i.e., at this point the SFCL does not need to be triggered to protect this branch. The same argument applies to the domes-

tic branch under Fault 1 and Fault 3 conditions. Our results are presented below in terms of the single or multiple SFCL strategies.

### 4.1 Single SFCL installation

Fig.7 (a) shows the reduction in fault current under the three fault conditions illustrated in Fig. 1 when a single SFCL is installed at at the referred locations (Location 1 to 5). For the sake of comparison, the size of the superconductor which has to be defined into the $E-J-T$ power law model, has been systematically adjusted so that it allows to define the same maximum resistance that the one used with the step resistance model. Thus, when the step resistance model is considered, the maximum reduction of the fault current is overestimated in comparison with the more realist $E-J-T$ model, i.e., for all the 5 SFCL locations the first peak of the fault current was always found to be lower in the first case. The reason to this difference is that, once the current exceeds the critical value of the SC, the SFCL described by the step resistance directly jump to the maximum resistance after the pre-defined response time, whilst in the $E-J-T$ model the dynamic increase of the resistance depends not only on the passing current, but also on the temperature of the superconductor. Therefore, under the $E-J-T$ model the SFCL cannot gain its maximum rated resistance before the first fault peak is reached, which leads to a relatively lower reduction of the fault current ($\sim 20\%$).

Based on both SFCL models tested, the simulations performed generally show a negative impact on the reduction of the fault peak at certain integration points when the SFCL is installed at Location 1 or Location 2, i.e., on these cases the fault current actually increase by the insertion of a SFCL. In more detail, when the SFCL is installed besides the wind farm (Location 2), a sudden increase of fault current flowing through the integrating point under the Fault 2 (at the domestic branch) is caused by the abrupt change of power system's impedance. This SFCL enters the normal state reducing the current output of the wind farm due to its rapid rise in resistance and hence, the conventional power plant and the upstream power grid are forced to supply higher current to the faulted branch. Similar behaviour is obtained under the fault conditions F1 and F2 when the SFCL is installed at Location 2, and the current is measured at the integrating point (see Fig. 7 (a) & Fig. 1). Furthermore, it should be noticed that when a single SFCL is installed at Location 1 (integrating point), following the $E-J-T$ model the SFCL can only limit the fault current in two cases, whilst with the simplified step-resistance the benefits of the SFCL can be overrated as it leads to a positive balance in up to four different fault conditions. This fact highlights the importance of finding a suitable optimal allocation strategy for the SFCLs under a wide number of fault conditions, and the need of considering adequate physical properties for the electro-thermal dynamics of the SC materials. It ultimately tries to fill the gap between the acquired scientific knowledge and the demand of more reliable information from the standpoint of the power distribution companies. Thus, the final decision for an optimal location has to be made under the circumstance of having a twofold conclusion.

Firstly, the decision can be made accordingly to the highest total reduction on the fault current passing through different points and under different fault circumstances as shown in Fig. 7 (a). There, it can be observed that for the eight most important cases combining the occurrence of a fault at certain positions and the measuring point for the current reduction, the SFCL installed at the port of the wind farm (Location 2) results to be the best option, as in this case the fault current can be reduced in six of the eight different scenarios with an accumulated reduction of 290% from the step resistance model, and 220% from the $E-J-T$ power law model, respectively. Nevertheless, it is to be noticed that this strategy has also an adverse impact on the remaining two other scenarios (F1-IP & F2-IP). Secondly, a decision can be made in terms of the overall performance for achieving positive impact under the scope of any of prospective circumstances. In this sense, we have determined that placing the SFCL at the Location 5, i.e, at the bus-tie between the industrial and domestic branches, is the most reliable option. Furthermore, by considering this strategy it is worth mentioning that the SFCL is capable of reducing the harmonics and voltage dips, doubling the short-circuit power, and ensuring even loading of parallel transformer. Moreover, the recovery characteristics of the SFCL can also see benefit from this arrangement as after a quench of the SFCL, the bus-tie can be switched open for a short time (few seconds) to help the SFCL restoring the superconducting state. However, a drawback of the switching strategy is that this measure may temporarily reduce the quality of the power supply, but a strong impact on the normal operation of the power system is not foreseen.

### 4.2 Multiple installation of SFCLs

Firstly, a double protection strategy, i.e, the installation of two SFCLs in different grid positions has been assessed. According to both, the step resistance model and the $E-J$ power law based model, the highest

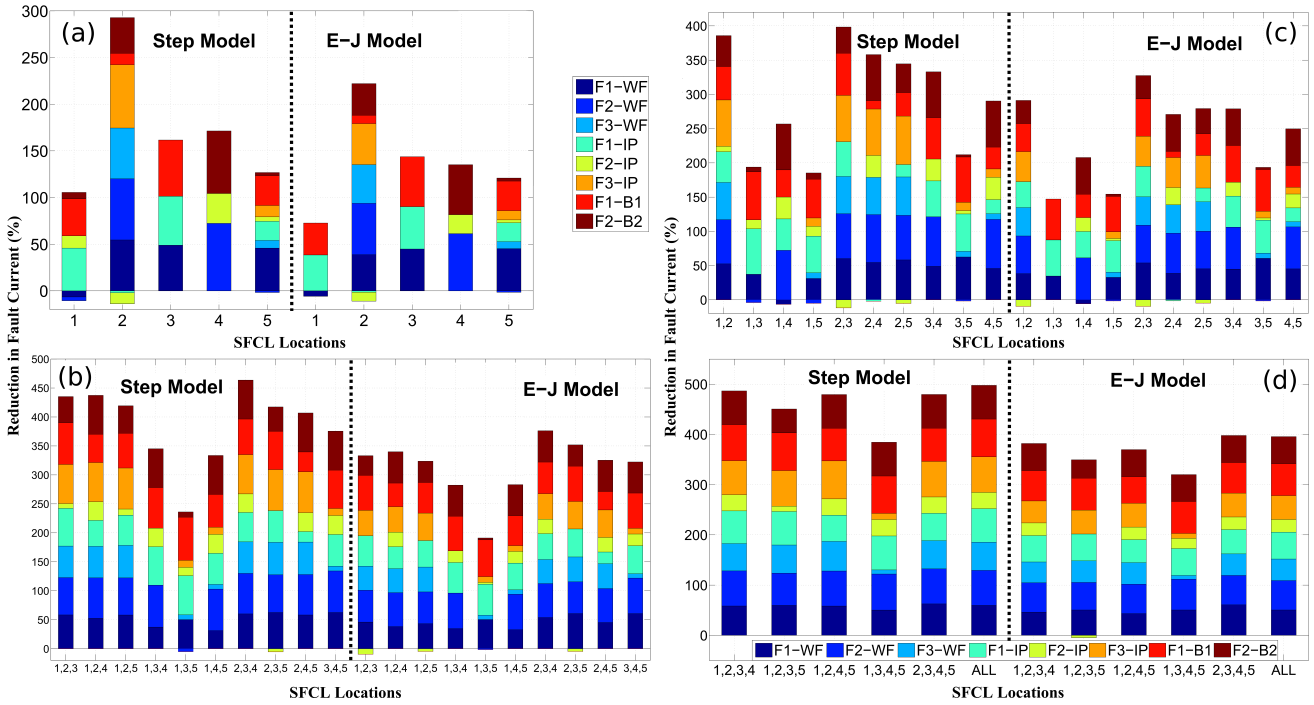


**Fig. 7** (Color Online) Reduction of the first peak of fault current events at different locations, measured after the installation of a (a) single SFCL, (b) two SFCLs, (c) three SFCLs, and (d) up to four and five SFCLs installed at different locations.

fault current reduction was always achieved when the SFCLs are installed at Location 2 (wind farm) and Location 3 (industrial branch) simultaneously, accomplishing a 400% and 330% total fault limitation respectively (Fig. 7 (b)). Indeed, this arrangement can be considered as a much better strategy in comparison with the results obtained when just a single SFCL is considered, as the total current limitation is improved by $\sim 110\%$. Furthermore, contrary to the previous case, the current flowing through the integrating point when the fault occurs at the industrial branch (Fault 2) significantly decreases rather than having an adverse effect onto the power system. Moreover, it is to be noticed that under this dual strategy the measured current reduction shows a balanced performance on all the different analysed cases, unlike the results obtained for when a sole SFCL is installed. On the other hand, if the system operators measure the optimal strategy for the installation of the two SFCLs in terms of the number of limited cases, different conclusions can be obtained under the framework of different physical models, e.g., when the step-resistance or $E-J-T$ power law model is considered. On the one hand, according to the step resistance model, installing the two SFCLs at Locations 1 & 2 or Locations 4 & 5 both can positively response to all eight measured fault conditions. In fact, when the SFCLs at Locations 1 & 2 are considered, a better performance is obtained as the total reduction in the fault current achieved is 40% greater than the performance obtained when the SFCLs are installed at Locations 4 & 5 (290%), respectively. On the other hand, when the $E-J-T$ model is assumed, installing the SFCLs at the Locations 1 & 2 would increase the magnitude of current at the integrating point under the occurrence of a fault in the domestic branch (Fault 2). It is due to the unsuccessful triggering of the SFCL at Location 1 as explained in the previous subsection. Therefore, from the point of view of the system operators, the Locations 4 & 5 can be considered as the most reliable solution as it is the only combination capable to limit all fault conditions and in all the considered scenarios.

Secondly, we have added an additional SFCL to the grid, and we have assessed overall performance of this new system. Thus, as it is shown in Fig. 7 (c), most installation strategies of three SFCLs allow the reduction of the fault current at all eight measured scenarios. Both SFCL models agree with the conclusion that the highest decrement in the fault current is achieved when the SFCLs are installed at the Locations 2, 3 and 4, simultaneously. This strategy shows a 470% total reduction in the case of the step resistance model, and 375% for the case of the $E-J-T$ model, i.e., attaining a significant increase on the overall performance of the system by about a 70% and 45% factor, respectively, it in comparison with the best achieved performance when the dual SFCLs strategy was considered. Besides

this remarkable improvement, the three SFCLs strategy can further response positively to any fault conditions, which means that for the concomitant decision between the current reduction criteria and the number of cases exhibiting fault current reduction, the choice for the three SFCLs strategy can be considered as the most reliable one. Nevertheless, until a significant reduction of the overall price of a SFCL will not be achieved, the distribution network operators could consider that this strategy may not be cost-effective in terms of the initial investment, but given the expected reduction on the prices of the second generation of high temperature superconducting wires, this decision can be seen as the most profitable strategy in terms of the grid safety and reliability. However, a limit for the maximum number of the SFCLs required must also be established in order to guarantee minimum costs with maximum benefits.

Thus, in Fig. 7 (c) we show the performance comparison among five different scenarios when four SFCLs are installed into the power system. On the one hand, with four SFCLs working together, all combinations can effectively limit the fault current for all eight studied cases excepting when the SFCLs are described by the $E-J-T$ model and the SFCLs are installed at Locations 1, 2, 3, and 5, simultaneously. Under this scheme the measured fault current increases when the fault is initialised at the domestic branch (Fault 2), due to the no action of the SFCL installed at Location 1. On the other hand, it is to be noticed that when the step resistance model is considered, the accumulated maximum reduction on the fault current is again overestimated, achieving a 480% reduction when the SFCLs are installed at the set of Locations $(1, 2, 3, 4)$ or $(2, 3, 4, 5)$, in comparison with a prospective reduction of 395% at Locations $(2, 3, 4, 5)$ when the most realist $E-J-T$ model is considered. In fact, even with the concurred action of up to 4 SFCLs, we have obtained that the accumulated maximum reduction on the fault current is just over a 10% more than in the previous case (3 SFCLs), which allows to define an upper limit for the number of SFCLs needed.

In order to verify our previous statement, we have studied also the influence of considering even one more SFCL, as there is a total of five prospective locations for the SFCLs in the power grid displayed in Fig. 1. Compared with the last analysed case (4 SFCLs), the accumulated maximum reduction on the fault current has reached just a 15% more increase when the SFCLs are based upon the step resistance model, but outstandingly no further improvement has been obtained when the more realistic $E-J-T$ model was incorporated. This important result can be understood as a consequence of the mutual influence between the integrated SFCLs, i.e., when the fault current passing through one SFCL is substantially decreased by the influence of the others, the rate of heat accumulation slows down accordingly, leading to deceleration of the temperature rising and hence to a reduction of the resistance that the SFCL can develop before reaching the first peak of the fault.

Summarising, in Table 1 the optimal allocation strategies and the corresponding performances of the SFCLs obtained during our study are presented. The preferable locations for the installation of the SFCLs have been determined in terms of the two identified standards: $(i)$ the maximum accumulated fault current reduction and, $(ii)$ the maximum number of measuring conditions that could be limited. The results are categorised by the number of SFCLs that the system operators could want to install, and also the physical models that emulate the characteristics of the SFCLs. It is worth noting that in all the cases the step resistance model leads to an overestimation of the actual performance figures that may be offered by the SFCLs when more realistic physical properties are considered. Finally, we want to call the attention of the readers on the fact that when the strategy for maximising benefits is installing a sole or two SFCLs, compromise has to be made between increasing the fault current reduction and the actual number of measuring conditions where the fault current can be limited. Therefore, based upon the comprehensive study presented in this paper, we conclude that the optimal installation strategy refers to the installation of maximum 3 SFCLs at the Locations 2, 3, and 4, as for this case a maximum reduction of the fault current is achieved for all fault conditions, and furthermore, the adding of more SFCLs does not represent a significant improvement to be concurrent with the minimisation of costs.

## 5 Conclusion

The superconducting fault current limiter is a promising device to limit the escalating fault levels caused by the expansion of power grid and integration of renewables. This paper presents a comprehensive study on the performance and optimal allocation analysis of resistive type SFCLs inside of a power system with an interconnected wind farm, built from the base of the UK network standards. In order to unveil the impact of the superconducting material properties on the decision making for installing SFCLs, two different models have been considered throughout the study. Firstly, the active operation of the SFCL has been modelled by means of a step resistance or Heaviside function which

**Table 1** Optimal installation strategies for SFCLs according to the step-resistance and E-J power law models. The maximum fault current reduction (FCR) value (per case) has been calculated as the sum of the percentage reductions of the fault current measured at the wind farm output, the integrated point, and branches 1 and 2, for the three fault conditions shown in Fig. 1. It is worth noticing that, not at all measuring locations the fault current is reduced (see Fig. 7). Therefore, the table also shows the values for the accumulated fault current reduction when the fault current is reduced in a greater number of measuring conditions.

| **Step-Resistance Model** | | | | | |
|---|---|---|---|---|---|
| Maximum Fault Current Reduction (%): | 290 | 400 | 470 | 480 | 495 |
| No. of measuring conditions with/without FCR: | 6 / 2 | 7 / 1 | 8 / 0 | 8 / 0 | 8 / 0 |
| Number of installed SFCLs: | 1 | 2 | 3 | 4 | 5 |
| SFCLs's Locations: | 2 | 2, 3 | 2, 3, 4 | 1, 2, 3, 4[1] | 1, 2, 3, 4, 5 |
| No. of measuring conditions with/without FCR: | 7 / 1 | 8 / 0 | 8 / 0 | 8 / 0 | 8 / 0 |
| Accumulated FCR (%) for Max. No. of measuring conditions: | 130 | 330 | 470 | 480 | 495 |
| Number of installed SFCLs: | 1 | 2 | 3 | 4 | 5 |
| SFCLs's Locations: | 5 | 1, 2 | 2, 3, 4 | 1, 2, 3, 4 | 1, 2, 3, 4, 5 |
| **E-J Power Law Model** | | | | | |
| Maximum Fault Current Reduction (%): | 220 | 330 | 375 | 395 | 395 |
| No. of measuring conditions with/without FCR: | 6 / 2 | 7 / 1 | 8 / 0 | 8 / 0 | 8 / 0 |
| Number of installed SFCLs: | 1 | 2 | 3 | 4 | 5 |
| SFCLs's Locations: | 2 | 2, 3 | 2, 3, 4 | 2, 3, 4, 5 | 1, 2, 3, 4, 5 |
| No. of measuring conditions with/without FCR: | 7 / 1 | 8 / 0 | 8 / 0 | 8 / 0 | 8 / 0 |
| Accumulated FCR (%) for Max. No. of measuring conditions: | 120 | 250 | 375 | 395 | 395 |
| Number of installed SFCLs: | 1 | 2 | 3 | 4 | 5 |
| SFCLs's Locations: | 5 | 4, 5 | 2, 3, 4 | 2, 3, 4, 5 | 1, 2, 3, 4, 5 |

is initialised by a set of preallocated parameters. Secondly, a most realistic model for the operation of the SFCL taking into consideration the proper $E-J$ characteristics of the superconducting material with dynamic temperature evolution has been considered. We have proven that SFCL technologies can effectively improve the damping characteristics of the generation system, and mitigate voltage dips at the grid, independently of the assumed model. However, we have demonstrated that despite a significant reduction on the time computing can be achieved when models of the step-resistance kind are considered, such simplifications lead to strong overestimations of the actual prospective performance of the SFCL, it in terms of the maximum reduction on the fault current and its correlated normal resistance. Furthermore, a complementary protection scheme for preventing the burning of the SFCL has been implemented together with the $E-J$ power law based model, what improves significantly the recovery of the SFCL during the transient states after a fault event.

Then, a systematic study on the prospective strategies for the installation of a sole or multiple SFCLs has been performed. Thence it has been proven that the concomitant cooperation of three SFCLs each installed at the Locations 2, 3, and 4, respectively, can be seen as the best protection strategy in terms of both the performance and the reliability figures of the overall grid within a minimum investment scheme vs maximum benefit. For achieving this conclusion all the potential combinations between two, three, four, and five SFCLs have been studied under a wide number of fault scenarios and measuring strategies.

## Acknowledgement

This work was supported by the Engineering and Physical Sciences Research Council (EPSRC), project NMZF / 064. X. Zhang acknowledges a grant from the China Scholarship Council (No. 201408060080).

## References

1. Hartikainen T., Mikkonen R., and Lehtonen J.: Appl. Energ. **84** 29 (2007)
2. Zhang J., *et al.:* IEEE Trans. Ind. Electron. **23** 5601705 (2009)
3. Kovalsky L., Yuan X., Tekletsadik K., Keri A., Bock J., and Breuer F.: IEEE Trans. Appl. Supercond. **15** 2130 (2005)
4. Ye L., and Juengst K.-P.: IEEE Trans. Appl. Supercond. **14** 839 (2005)

5. Ruiz H.S., Zhang X., and Coombs T.A.: IEEE Trans. Appl. Supercond. **25** 5601405 (2015)
6. Khan U.A., Seong J., Lee S., Lim S., and Lee B.: IEEE Trans. Appl. Supercond. **21** 2165 (2011)
7. Hwang J.-S., Khan U.A., Shin W.-J., Seong J.-K., Lee J.-G., Kim Y.-H., and Lee B.-W.: IEEE Trans. Appl. Supercond. **23** 5600204 (2013)
8. Park W.-J., Sung B.C., and Park J.-W.: IEEE Trans. Appl. Supercond. **20** 1177 (2010)
9. Park W.-J., Sung B. C., Song K.-B., and Park J.-W.: IEEE Trans. Appl. Supercond. **21** 2153 (2011)
10. Langston J., Steurer M., Woodruff S., Baldwin T., and Tang J.: IEEE Trans. Appl. Supercond. **15** 2090 (2005)
11. Colangelo D., and Dutoit B.: IEEE Trans. Appl. Supercond. **23** 5600804 (2013)
12. UK Electricity Networks. In parliamentary Office of Science and technology, number 163, October (2001)
13. Feng Y., Tavner P., and Long H.: Proceedings of the ICE-Energy **163** 167 (2010)
14. Blair S.M., Booth C.D., and Burt G.M.: *IEEE Trans. Appl. Supercond.* **22** 5600205 (2012)
15. Sung B.C., Park D.K., Park J.-W., and Ko T.K., IEEE Trans. Ind. Electron. **56** 2412 (2009)
16. Alaraifi S., Moursi M.E., and Zeineldin H.: IEEE Trans. Power Syst. **28** 4701 (2013)
17. Buhl D., Lang T., and Gauckler L.: Supercond. Sci. Technol. **10** 32 (1997)
18. Paul W., and Meier J.: Physica C **205** 240 (1993)
19. Herrmann P., Cottevieille C., Leriche A., and Elschner S.: IEEE Trans. Magn. **32** 2574 (1996)
20. Bock J., Breuer F., Walter H., Elschner S., Kleimaier M., Kreutz R., and Mathias N.: IEEE Trans. Appl. Supercond. **15** 1955 (2005)
21. Noe M., Juengst K.-P, Werfel F., Cowey L., Wolf A., and Elschner S.: IEEE Trans. Appl. Supercond. **11** 1960 (2001)
22. Paul W., Chen M., Lakner M., Rhyner J., Braun D., and Lanz W.: Physica C **354** 27 (2001)
23. Chen M., Paul W., Lakner M., Donzel L., Hoidis M., Unternaehrer P., Reto W., and Michael M. *Physica C* **372** 1657 (2002)
24. Elschner S., Breuer F., Wolf A., Noe M., Cowey L., and Bock J.: IEEE Trans. Appl. Supercond. **11** 2507 (2001)
25. Rhyner J.: Physica C **212** 292 (1993)
26. Aly M.M., and Mohamed E.A.: Comput. Eng. Syst. 227 (2012)
27. Slawomir K., Tadeusz J., Beata K.-K., Janusz K., and Grzegorz W.: IEEE Trans. Appl. Supercond. **15** 2098 (2005)
28. Rettelbach T., and Schmitz G.: Supercond. Sci. Technol. **16** 645 (2003)
29. Noe M., and Steurer M.: Supercond. Sci. Technol. **20** R15 (2007)
30. Bock J., Breuer F., Walter H., Noe M., Kreutz R., Kleimaier M., Weck K.H., and Elschener S.: *Supercond. Sci. Technol.* **17** S122 (2004)
31. Meerovich V., and Sokolovsky V.: Supercond. Sci. Technol. **20** 457 (2007)
32. Blair S.M., Booth C.D., Singh N.K., Burt G.M., and Bright C.G.: *IEEE Trans. Appl. Supercond.* **21** 3452 (2011)
33. Morandi A.: Physica C **484** 242 (2013)
34. Kundur P., Balu N.J., and Lauby M.G.: Power system stability and control. New York: McGraw-Hill (1994)
35. Melhem Z.: High temperature superconductors (HTS) for energy applications. Woodhead Publishing Ltd., (2011)